New Conducted Electrical Weapons: Finite Element Modeling of Safety Margins

Dorin Panescu, Ph.D., *Fellow IEEE*, Mark W. Kroll, Ph.D., *Fellow IEEE*,
and Michael A. Brave, M.S., J.D., *Sr. Member IEEE*

***Introduction*—We have previously published on the ventricular fibrillation (VF) risk with TASER® X26 conducted electrical weapon (CEW). Our risk model accounted for realistic body mass index distributions, modeled the effects of partial or oblique dart penetration, and used epidemiological CEW statistics. As new CEWs have become available to law enforcement, their cardiac safety profile was not quantified. Therefore, we applied our VF probability model to evaluate their cardiac risk.**

***Methods and Results*—An eXperimental Rotating-Field (XRF) waveform CEW and the X2 CEW are new 2-shot electrical weapon models designed to target a precise amount of delivered charge per pulse, 64 µC and 62 µC, respectively. They can deploy 1 or 2 probe pairs, delivered by 2 separate cartridges. New Smart Probes (SP), which carry 11.5 mm long CEW darts, can be used with XRF and X2 CEWs. Finite element modeling (FEM) was used to approximate the current and charge densities produced by XRF and X2 CEWs in tissues located in the vicinity of darts, including accounting for the effects of fat, anisotropic skeletal muscles, sternum, ribs, and lungs. Using our previous cardiac risk probabilistic model, the new XRF and X2 CEWs operated with 11.5 mm SPs, had an estimated overall theoretical VF risk of less than 1 in 1 300 000 and 1 in 1 490 000 cases, respectively. We also found that the XRF and X2 CEWs had increased cardiac safety margins with respect to those previously reported for the X26 CEWs when all three CEW models were operated with 9 mm CEW darts. Lastly, the cardiac risk of these new CEWs (< 0.76 ppm) was found to be much lower than reported levels of CEW non-cardiac fatal injuries (e.g. falls and burns, > 7.2 ppm).**

***Conclusions*—While not risk-free, the new TASER XRF and X2 CEWs offer increased cardiac safety margins and extremely low cardiac risk profiles.**

Keywords: Cardiac Risk, CEW, Fibrillation, Finite Element Model, TASER.

I. Introduction

Conducted electrical weapons (CEWs) are popular law enforcement, military, and civilian force options. We have previously published on the cardiac fibrillation risk with the TASER® X26 CEW [1]. Our risk model accounted for realistic body mass index (BMI) distributions, used a new model of effects of partial or oblique dart penetration and factored in epidemiological CEW statistics [1]. Two new next-generation Smart-Weapon CEWs, the eXperimental Rotating-Field (XRF) waveform CEW, which is in development, and the X2 CEW, already available, have been studied. Both the XRF and X2 CEWs utilize charge metering and pulse calibration to target a precise amount of delivered charge per pulse, 64 µC and 62 µC, respectively [2, 3]. They use electronic circuits to measure the charge delivered by the previous pulse. The targeted charge delivery of the next pulse is then controlled accordingly so that it is tightly adjusted toward the specified charge value. Both CEWs use 2 cartridge bays in order to provide for immediate back-up shots, if determined necessary by the deploying officer.

The XRF CEW drives electrical stimuli along 4 field vectors in a rotating sequence, as illustrated in Fig. 1. The dart numbers correspond to the cartridge bay number. First pulse of the sequence is delivered between darts 1+ and 1-. Second pulse of the sequence goes from dart 1+ to dart 2-. Third pulse is applied between darts 2+ and 2-. Fourth pulse crosses from dart 2+ to dart 1-. Then the sequence repeats itself. There are 11 pulses per second (pps) delivered across each of the 4 vectors. Hence, under normal operation, each dart discharges at a rate of 22 pps.

Figure 1. Rotating pulse-drive sequence for the XRF CEW (figure shows an illustration of a CEW, not the actual XRF CEW).

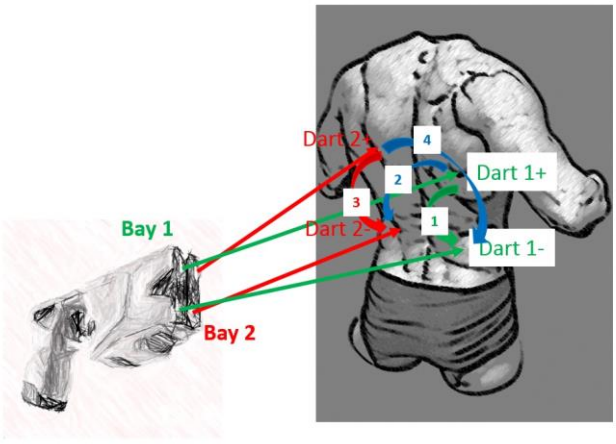

The rotating pulse-drive sequence is designed to increase XRF weapons efficacy. Even when XRF is deployed from a

D. Panescu is Chief Technical Officer, Vice President R&D at HeartBeam, Inc. (e-mail: panescu_d@yahoo.com). Dr. Panescu is a paid consultant to Axon Enterprise, Inc. (Axon), [formerly TASER International, Inc. (TASER)].

M. W. Kroll is an Adjunct Professor of Biomedical Engineering at the University of Minnesota, Minneapolis, MN (e-mail: mark@kroll.name). Dr. Kroll is a consultant to Axon, and a member of the Axon Scientific and Medical Advisory Board (SMAB) and Corporate Board.

M. A. Brave is Manager/Member of LAAW International, LLC, and is an employee of Axon, Director of the Axon Science and Medical Research Group, and legal advisor to the Axon SMAB and the Axon Training Advisory Board (e-mail: brave@laaw.com).

All authors have served as expert witnesses for Axon or law enforcement.

Authorized licensed use limited to: Charles University. Downloaded on October 10 2025 at 23:49:05 UTC from IEEE Xplore. Restrictions apply.

closer distance to a subject, the cross vectors #2 (darts 1+ to 2-) and #4 (darts 2+ to 1-) are likely to have a dart spread greater than 30 cm, a distance which has been empirically found to produce a more efficacious motor-nerve mediated muscular effect [4].

Additionally, new Smart Probes (SP), with 11.5 mm CEW darts, have been released for law enforcement use. The darts of these Smart Probes have been newly designed and are 2.5 mm longer than the older 9 mm CEW darts, and 1.5 mm shorter than the XP darts. The SPs are expected to be more effective in penetrating through, and adhering to, subjects' clothing.

In this study, we applied the previously published cardiac safety probabilistic model to evaluate the ventricular fibrillation (VF) risk of these two new next-generation Smart-Weapon CEWs, the XRF CEW and the X2 CEW when operated with 11.5 mm Smart Probes.

II. Methods

A. Summary of the CEW cardiac risk probabilistic model

Our VF risk probabilistic model was described in detail previously [1]. In summary, computing CEW cardiac risk involved the following steps:

1. Estimate applicable CEW thresholds for VF (VFT);
2. Use Finite Element Modeling (FEM) to estimate the maximal distance from the tip of a CEW dart to the tissue region (MaxDTH) still exposed to the VFT charge levels. The analyses included realistic tissue types around the dart (e.g. fat, sternum, ribs, intercostal muscle and lungs) and their electrical material properties, including the anisotropy of the skeletal muscle;
3. Estimate the skin-to-heart distance (STH) required for VF induction;
4. Estimate the effects of oblique skin penetration angles of CEW darts on STH;
5. Based on published BMI distributions, compute the probability of a subject having a STH in the range required for VF induction;
6. Based on epidemiological data, compute the probability of a subject being hit by CEW darts in the chest region having narrow STH;
7. Compute overall CEW cardiac risk; and
8. Correlate with existing epidemiological statics for consistency.

B. XRF and X2 CEWs output parameters and VFTs

Figures 2 and 3 show the output current and voltage waveforms of the XRF and the X2 CEWs. Table I summarizes XRF and X2 CEWs electrical output parameters relevant to cardiac risk analyses. Formulas (1) and (2) apply the VF-induction strength-duration theory to compute the thresholds for direct VF induction by XRF and X2 CEWs. We have previously explained these formulas in detail [1]. They were based on extensively published data [5 – 10].

The current density VFTs were:

$$XRF\_VFT_J = 7\ mA/cm^2*(1+1.2\ ms/0.05\ ms) = 175\ mA/cm^2 \quad (1a)$$

$$X2\_VFT_J = 7\ mA/cm^2*(1+1.2\ ms/0.066\ ms) = 134\ mA/cm^2 \quad (1b)$$

TABLE I. Relevant output parameters of TASER XRF and X2 CEWs.

Parameter	XRF	X2
Open-circuit peak voltage [kV]	50	52
Average Pulse Voltage [V]	770	560
Peak Main Phase voltage in typical load [kV]	1.7	1.2
Peak Main Phase current in typical load [A]	2.8	2
Energy delivered in typical load [J/pulse]	0.098	0.069
Power into 600 ohm load [W]	2.15	1.3
Net charge in the main phase [μC]	64	62
Impulse duration [μs]	50	66
Pulse rate [pulse/s]	22	19

Figure 2. TASER XRF and X2 CEW current waveforms.

Figure 3. TASER XRF and X2 CEW voltage waveforms.

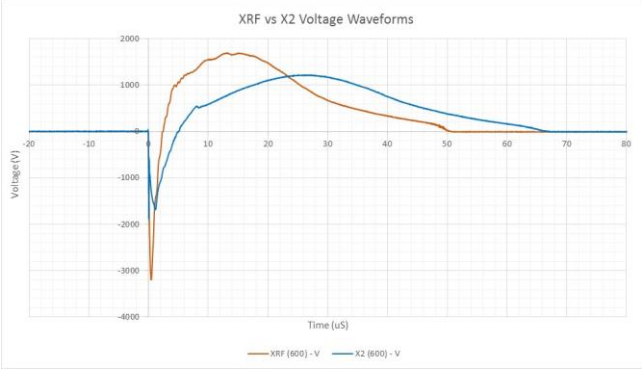

Correspondingly, the charge density threshold for VF induction were computed as:

$$XRF\_VFT_Q = 7\ mA/cm^2 * 0.05\ ms * (1+1.2\ ms/0.05\ ms) = 8.75\ \mu C/cm^2 \quad (2a)$$

$$X2\_VFT_Q = 7\ mA/cm^2 * 0.066\ ms * (1+1.2\ ms/0.066\ ms) = 8.86\ \mu C/cm^2 \quad (2a)$$

Sugimoto *et al.* suggested that VFTs drop with an increasing number of captured premature ventricular responses [11 – 13]. With 4 captured premature ventricular responses, the VFT may drop to about 3 times the cardiac cell excitation threshold. We used the term premature ventricular response VFT (pvrVFT) to separate this reduced threshold from the VFT discussed above. Using the above rheobase and chronaxie, we computed $pvrVFT_J$ and $pvrVFT_Q$:

$$XRF\_pvrVFT_J = 3*1.48\ mA/cm^2*(1+1.2\ ms/0.05\ ms)$$

Authorized licensed use limited to: Charles University. Downloaded on October 10,2025 at 23:49:05 UTC from IEEE Xplore. Restrictions apply.

= 111 mA/cm^2 (3a)

$X2\_pvrVFT_J$ = 3*1.48 mA/cm^2*(1+1.2 ms/0.066 ms)
= 85 mA/cm^2 (3b)

XRF_pvrVFT_Q = 3*1.48 mA/cm^2 * 0.05 ms * (1+1.2 ms/0.05 ms)
= 5.55 μC/cm^2 (4a)

$X2\_pvrVFT_Q$ = 3*1.48 mA/cm^2 * 0.066 ms * (1+1.2 ms/0.066 ms)
= 5.62 μC/cm^2 (4b)

C. Finite Element Models for MaxDTH computations

We used 3-D FEM to understand the current density distributions generated by CEW electrodes [14]. Thoracic tissue distributions were for a thin body (Figs. 6 and 8):

- Tissue regions (dimensions reflect region thickness):
  - Skin: 2 mm thick
  - Fat: 6 mm thick
  - Pectoral Muscle: 7 mm thick
  - Sternum/Rib/Intercostal muscle: 11 mm thick
  - Lung and connective tissue: 8 mm thick
  - Cardiac tissue: 11 mm thick
- Model was 24 cm long, 20 cm wide and 4.5 cm thick
- Voltage boundary conditions: 1700 V (XRF) and 1200 V (X2)
- Model computed steady-state solution
- CEW dart electrodes – 9 or 11 mm long, 1 mm diameter, embedded in tissue up to full length, 15 cm apart.
- Elements: 36480 hexahedral elements, spatial resolution 0.17 – 2.75 mm.

The distribution of tissues and their dimensions were based on data from anatomic atlases and visible human databases [15 – 17].

Table II shows the FE region resistivities, which were based on previous published reports [18 – 21].

TABLE II. FEM material properties.

Region	**Resistivity [Ω·cm]**
Skin	5000
Fat	2500
Pectoral muscle	ρ_x = 1000; ρ_y=ρ_z=200
Bone (sternum, rib)	1 000 000
Intercostal muscle	ρ_x = 1000; ρ_y=ρ_z=200
Lung	1500
Connective tissue	500
Cardiac tissue	333
Electrode	0.001

MaxDTH was defined as the distance from the dart tip to the farthest element that had a current density greater than VFT_J and was mapped around the CEW dart tip. Alternatively, MaxDTH was also computed and discussed based on charge density distribution and thresholds, VFT_Q. The model was also used to analyze the current attenuation effects of fat, anisotropic skeletal muscle, sternum and rib layers had on MaxDTH. To account for the worst-case scenario, we chose the XRF and X2 peak main-phase voltages, 1700 V and 1200 V, respectively, as boundary conditions, rather than the pulse-averaged voltages.

D. STH vs. BMI distributions

The distance between the skin surface and the corresponding closest point on the heart, abbreviated MinSTH, depends on the subject's BMI. This dependency was studied in detail by the Wisconsin and Cleveland groups [22, 23]. Figure 4a shows the distribution MinSTH vs. BMI measured using echocardiographic imaging by the Wisconsin group in 55 male subjects [22]. Figure 4b shows the MinSTH vs. BMI relationship, as measured using computer tomography (CT) by the Cleveland group in 37 males [23].

Figure 4a. Wisconsin group MinSTH vs. BMI and ARD subject BMI range [22].

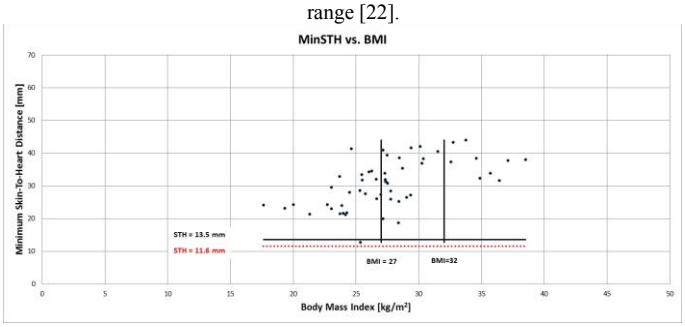

Figure 4b. Cleveland group MinSTH vs. BMI and ARD subject BMI range [23].

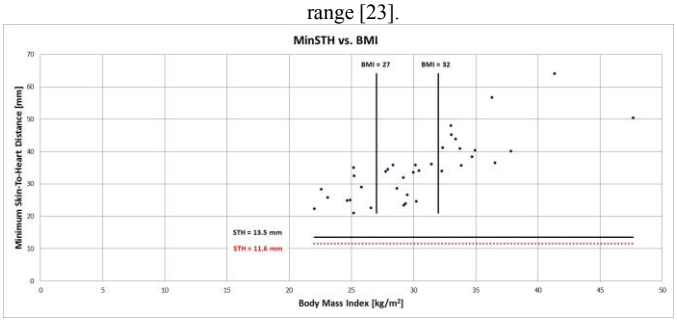

Males are by far the best represented gender during encounters with law enforcement that result in deployment of CEWs [24]. Both Figs. 4a and 4b mark the BMI range of 27 – 32 kg/m^2, corresponding to law enforcement temporal arrest-related death (ARD) subjects [24].

E. CEW chest shot distributions from epidemiological data

We used the previously published epidemiological data to compute the probability of CEW darts hitting the anterior chest (P_{chest}) and then the conditional probability to land at anterior chest locations where the heart is closest to the chest surface (P_{Zone_MinSTH}) [1]. Figure 5 illustrates the anterior chest area that was of interest for hit probability purposes. As in the past, we reviewed epidemiological studies in order to collect the relevant data [25 – 27]. We have also reviewed 24 cases in which CEW darts were deployed to the anterior chest. In all cases, the medical examiner reports or autopsy data were used to document the actual location of the CEW darts and the amount and angle of their penetration through the skin or chest wall.

Authorized licensed use limited to: Charles University. Downloaded on October 10,2025 at 23:49:05 UTC from IEEE Xplore. Restrictions apply.

Figure 5. CEW chest shot probabilities estimates took into account the approximate location of the heart in a subject's chest [26].

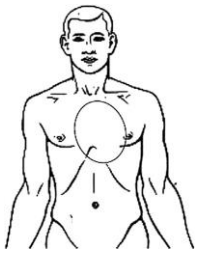

F. Cardiac risk computation

The same cardiac risk computation was employed, as previously published [1]:

$$VF_{risk} = P_{chest} * P_{Zone\_MinSTH} * P_{MaxDTHvsBMI} * P_{dart\_penetrate} \quad (5)$$

where:

- VF_{risk} is the overall probability of VF induction with the XRF or X2 CEWs;
- P_{chest} is the probability of hitting the anterior chest with CEW darts, as per cited epidemiological studies;
- P_{Zone_MinSTH} is the conditional probability of hitting the area of minimum STH, assuming the CEW dart landed on the anterior chest;
- $P_{MaxDTHvsBMI}$ is the probability of a subject having a STH shorter than the length of the CEW dart plus MaxDTH. This probability was computed based on the MinSTH vs. BMI distributions discussed in Figs. 4a and 4b; and
- $P_{dart\_penetrate}$ is the correction applied given that in the vast majority of cases CEW darts do not penetrate the skin in purely perpendicular mode and do not embed along their full length, even when hitting the MinSTH zone.

III. Results

A. MaxDTH to prevent VF induction

To evaluate the worst-case scenario VF risk, accounting for the Sugimoto effect, the FEM was used to analyze at what distance from the tip of CEW dart to the location where the current density dropped below $pvrVFT_J$. Assuming a CEW dart fully embedded into tissue, MaxDTH was 2.6 mm for the XRF and 2.5 mm for X2, respectively. Figures 6(a) and 6(b) illustrate the current density distribution around the tip of a CEW dart. Thus, under worst-case circumstances, for a 9 mm CEW dart, the STH would have to be at most 9 mm + 2.6 mm = 11.6 mm for the XRF and at most 9 mm + 2.5 mm = 11.5 mm for the X2. For greater STH, the residual CEW currents could not exceed pvrVF thresholds and VF could not be induced, including when considering the effects of premature ventricular responses. Figures 4a and 4b show STH distributions with respect to the 11.6 mm line. Note that none of the 92 patients had MinSTH less than 11.6 mm.

Figure 6(a). XRF CEW current density around a CEW dart fully embedded in tissue. Red zone area where current densities were > $pvrVFT_J$.

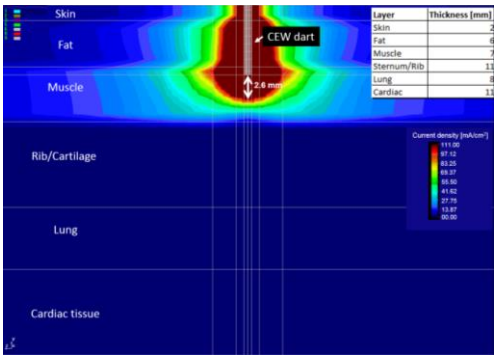

Figure 6(b). X2 CEW current density around a CEW dart fully embedded in tissue. Red zone area where current densities were > $pvrVFT_J$.

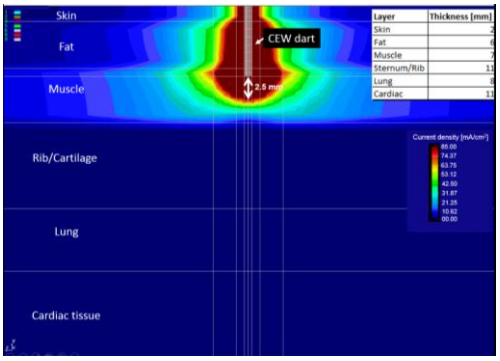

As such, when operated with 9 mm darts, both the XRF and the X2 CEWs were not expected to be capable of inducing VF in any of these patients. With Smart Probes, the minimal STH would have to be at most 11.5 mm + 2.6 mm = 14.1 mm for the XRF CEW and at most 11.5 mm + 2.5 mm = 14.0 mm for the X2 CEW. For greater STH, the residual CEW currents would not exceed pvrVF thresholds. Hence, VF could not be induced, including when considering the effects of premature ventricular responses. Figures 4a and 4b also show STH distributions with respect to the 14.1 mm line. Note that only one of the 92 patients had a MinSTH of 12.7 mm, which was less than 14.1 mm. As such, when operated with 11.5 mm SPs, assuming full and perfect perpendicular penetration through the skin, directly anterior to the heart, with no intervening clothing, the XRF or the X2 CEWs would have been hypothetically expected to be capable of inducing VF in only one of these 92 patients.

B. STH vs. BMI distributions

Based on data presented in Figs. 4a and 4b, we computed $P_{MaxDTHvsBMI}$. As defined above, this is the probability of a subject having a minimal STH shorter than 11.6 mm, for standard 9 mm darts, or shorter than 14.1 mm (XRF CEW) or 14.0 mm (X2 CEW), when 11.5 mm SPs were used. As seen in Figs. 4a and 4b, out of 92 volunteers, none had MinSTH ≤ 11.6 mm and only one experienced a MinSTH < 14.1 mm, or 12.7 mm to be precise. Hence, $P_{MaxDTHvsBMI\_9mm} = 0/92 = 0\%$ and $P_{MaxDTHvsBMI\_11.5mm} = 1/92 = 1.1\%$. The difference between 12.7 mm and 14.1 mm, or 1.4 mm, lies well within the imaging

Authorized licensed use limited to: Charles University. Downloaded on October 10,2025 at 23:49:05 UTC from IEEE Xplore. Restrictions apply.

instrumentation tolerance. Thus, it may very well be that none of the 92 volunteers exhibited a MinSTH effectively shorter than STH required to induce VF or pvrVF. Also, no volunteers with BMIs between 27 – 32 kg/m^2, such as those reported for ARD subjects, had STHs less than 14.1 mm. Hence, $P_{MaxDTHvsBMI}$ for practical, real field-use situations is much lower than 1/92.

C. Effects of partial or oblique-angle CEW dart penetration

In the vast majority of cases, CEW darts do not penetrate the skin in purely perpendicular mode, or do not embed along their full length. We deployed CEWs in gel phantoms simulating the human chest. Due to inertial effects, the darts penetrated only 6 mm, on average, much shorter than MinSTH distances observed in the cardiac imaging study. Therefore, it made sense to provide an estimate for a correction factor, $P_{dart\_penetrate}$, which adjusted the overall cardiac risk for incomplete or oblique CEW dart penetrations.

Figure 7 illustrates the trigonometry problem solved in order to correct for the CEW dart penetration angle, α, and for its partial penetration factor, k.

Figure 7. Diagram shows CEW dart entering the skin towards heart at an angle α and penetrating over a partial length, k*$Length_{dart}$.

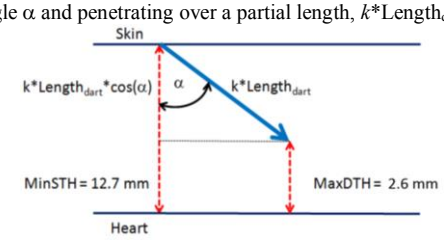

The geometric condition that must be met to induce VF equated to:

$$k*Length_{dart}*\cos(\alpha) + MaxDTH \geq MinSTH \quad (6)$$

where $0 \leq \alpha < \pi/2$ and $0 < k \leq 1$.

In other words, the sum of a partially penetrated CEW dart length projection onto the vertical axis plus the maximal distance from dart tip to the farthest VFT$_J$ or pvrVFT$_J$ contour (i.e. MaxDTH) must exceed MinSTH. For $Length_{dart}$ = 9 mm, there are no physical solutions to Eq. (6). Hence, as discussed before, under such circumstance the XRF and X2 CEWs would not be expected to induce VF in subjects according to the STH distribution revealed by the cardiac imaging study results discussed in section II.D. For $Length_{dart}$ = 11.5 mm α cannot exceed 27° for XRF CEW and 26° for X2 CEW (i.e. solution of (6) for k = 1). Forcing α = 0° provides the respective range for k. Hence, $10.1/11.5 < k \leq 1$ for XRF CEW and $10.2/11.5 < k \leq 1$ for X2 CEW. Where 12.7 mm – 2.6 mm (2.5 mm) = 10.1 mm (10.2 mm). Thus, the α and k ranges favorable to induction of pvrVF are:

$0 \leq \alpha \leq 27°$ and $10.1/11.5 < k \leq 1$ for XRF&11.5 mm SP

$0 \leq \alpha \leq 26°$ and $10.2/11.5 < k \leq 1$ for X2&11.5 mm SP

Outside these ranges, CEW darts are unlikely to present an effective penetration depth which were sufficiently close to the heart surface to induce VF. Solving for the probability that α and k fall within their respective range yields $P_{dart\_penetrate\_XRF}$ = 1.7% and $P_{dart\_penetrate\_X2}$ = 1.5%. As a note, we have not considered the reduction in penetration caused by subject's clothing. The subject's clothing may reduce, on average, the dart penetration depth by an additional minimum 1 – 2 mm. Even assuming just 1 mm penetration depth reduction due to clothing, there would be no physical solutions to Eq. (6) for either the XRF or X2 CEWs. Consequently, the correction factor $P_{dart\_penetrate}$ should be seen as a very conservative estimate.

D. Chest shot distributions from epidemiological data

Epidemiological studies provided data about the frequency of anterior chest hits during field uses of CEWs [25 – 27]. Out of 1201 consecutive TASER X26 CEW deployment cases, 178 cases involved dart locations on the anterior chest area shown in Fig. 5 [26]. None of these cases experienced documented VF events, or any other cardiac rhythm disturbance [26]. These deployments were prior to the manufacturer lowering the frontal preferred point of aim from center mass to lower center mass in September 2009. Thus, there is reason to assume that the above number for anterior chest shots would be smaller for XRF or X2 CEWs. Also, since the XRF and X2 probe deploying mechanism, distance and velocity are equivalent to those for the X26 CEW, we determined that our previous P_{chest} estimate of less than 14.8% can be used for this updated model. We have also reviewed 24 cases in which CEW darts contacted the anterior chest, in the approximate region circled in Fig. 5. In all cases, the respective medical examiner reports or autopsy data were used to document the actual location of CEW darts and the amount and angle of their penetration through the skin or chest wall. Out of 24 cases, 18 had their respective darts fall within the anterior chest area from Fig. 5. Out of these 2*18 = 36 dart locations, only one came close to the left chest region where the MinSTH distance could have been met. None of these cases had documented VF induction caused by CEW use. Thus, we estimated P_{Zone_MinSTH} to be less than 1/36, or 2.7%.

E. Overall cardiac risk with XRF and X2 CEWs

According to Eq. (5), if the XRF and X2 CEWs were used with 9 mm CEW darts, the theoretical overall cardiac risk would be extremely low because MinSTH distance conditions for VF induction (i.e. MinSTH = 12.7 mm – per Fig. 4) would not be met. With the XRF and X2 CEWs utilizing 11.5 mm SPs, the theoretical cardiac risk computed as (ppm stands for parts-per-million):

$VF_{risk\_XRF\_11.5mm}$ = 178/1201*1/36*1/92*0.017
= 0.000 000 76 = 0.76 ppm

$VF_{risk\_X2\_11.5mm}$ = 178/1201*1/36*1/92*0.015
= 0.000 000 67 = 0.67 ppm

equivalent to approximately 1 in over 1 300 000 cases for

Authorized licensed use limited to: Charles University. Downloaded on October 10,2025 at 23:49:05 UTC from IEEE Xplore. Restrictions apply.

XRF CEW and 1 in over 1 490 000 for X2 CEW.

IV. Discussion

We have previously employed this cardiac risk probabilistic model to estimate the theoretical probability of VF induction with TASER X26 CEWs with 9 mm darts [1]. With the X26 CEW, we determined that theoretical VF risk to be less than approximately 1 in 2 800 000 cases. Due primarily to pulse-metered and calibrated charge, the XRF and X2 CEWs deliver less charge than the X26 CEW with skin embedded darts. Also, the respective pulse durations are shorter. Hence, it was expected to find that the comparable cardiac risk was lower with these new charge-metered smart weapons. Indeed, with 9 mm darts, our model computed a cardiac risk of 0 for the XRF and X2 CEWs vs. 1 in 2 800 000 cases for the X26 CEW. This result can be explained by noting that the MaxDTH decreased from 4.3 mm for the X26 CEW to 2.6 mm and 2.5 mm for the XRF and X2 CEWs, respectively. These MaxDTH distances accounted for the VFT reduction caused by multiple premature ventricular responses, according to the Sugimoto effect [11 – 13]. As a consequence, if the XRF or X2 CEWs were operated with 9 mm CEW probes, the resulting electrical fields would not be expected to reach deep enough to trigger fatal cardiac rhythms, except, perhaps, in the thinnest subjects having extremely short STHs, far outside ranges documented by cardiac imaging [22 – 24]. If operated with the new, 11.5 mm smart CEW probes, the estimated theoretical VF risk for the XRF and X2 CEWs was 1 in more than 1.3 million cases, or less than 0.76 ppm. This remains a very low level of cardiac risk. Between 2011 and 2016, there were approximately 180 000 X2 CEWs sold in the United States [3]. At the time of this article, the XRF CEW has not yet been released to markets. Previous statistics gathered from the field use of TASER CEWs show an average of 0.55 field uses/year/sold CEW [27]. Hence, we estimated that, to-date, there have been approximately 235 000 field uses of Smart–Weapon CEWs. None of these have been confirmed to result in inducing cardiac arrest. While, at this time, the field use numbers are too low to support statistically significant conclusions, the trend is supportive and consistent with the VF risk estimated by our model.

Given that the XRF and X2 CEWs target a more precise control of the delivered pulse charge, it is important to discuss the implications of using charge density thresholds, VFT_Q, in estimating the cardiac risk. Figures 8(a) and 8(b) show the charge density profiles corresponding to XRF and X2 $pvrVFT_Q$, respectively. The $pvrVFT_Q$ thresholds are given in Eqs. 4(a) and 4(b), respectively. The corresponding MaxDTH distances, 1.75 mm (XRF CEW) and 1.67 mm (X2 CEW), are on the border of falling short of providing physical solutions for Eq. 6, including considering a dart length of 11.5 mm, such as for the new Smart CEW Probes. Under worst case scenario, assuming the entire 11.5 mm dart length has penetrated into tissue, Eq. 5 yields a charge-density-based VF risk of < 0.2 ppm. Therefore, the risk estimates provided in section III.E should be considered as highly conservative. Likely, real cardiac risks with XRF and X2 CEWs are likely significantly lower than the estimated < 0.76 ppm, perhaps even lower than 0.2 ppm.

Figure 8(a). XRF CEW charge density around a CEW dart fully embedded in tissue. Red zone area where charge densities were > $pvrVFT_Q$.

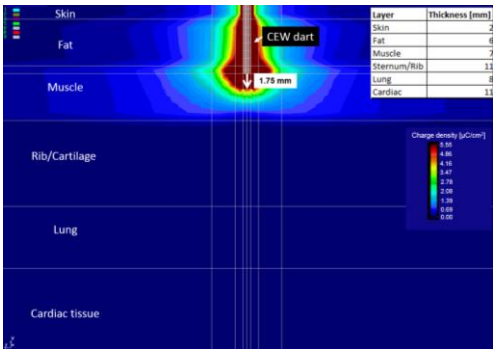

Figure 8(b). X2 CEW charge density around a CEW dart fully embedded in tissue. Red zone area where charge densities were > $pvrVFT_Q$.

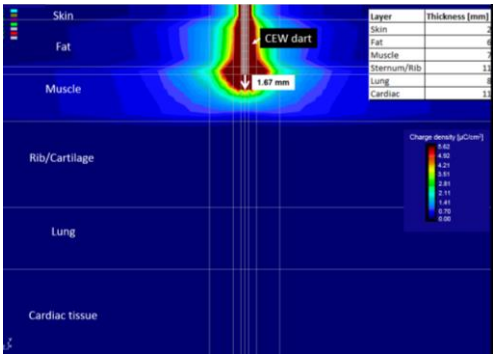

Non-cardiac CEW risk levels, such as injuries or death resulting from subjects' often uncontrolled fall during exposure to CEWs or such as fatalities caused by CEW igniting gasoline fumes, are much higher than the theoretical VF risks estimated above. Kroll et al. searched for ARD cases with TASER CEW usage where fall-induced injuries might have contributed to the death [28]. Their inclusion criteria were:

1. Arrest-related or in-custody incident;
2. Death occurred;
3. CEW was used in the incident;
4. Decedent fell during the incident;
5. Traumatic brain injury contributed to or caused the death.

The inclusion criteria were met in 24 cases. Of those, 5 were classified as "intentional" jumps (suicide or escapes) and another 3 cases were excluded because of missing contributing traumatic brain injury. In total, 16 cases with fatal brain injuries were found to be caused by falls resulting from use of CEWs. Compared to over 3 million cases of CEW field use, the resulting fatal fall risk was estimated at 5.3 ± 2.6 ppm [28].

There have been 6 fatal cases caused by CEWs igniting gasoline fumes or propane [29]. Over the estimated 3 million cases of CEW field use, the resulting fatal burn risk was estimated at 1.9 ppm [29, 30].

Authorized licensed use limited to: Charles University. Downloaded on October 10,2025 at 23:49:05 UTC from IEEE Xplore. Restrictions apply.

By comparison, our present study estimated the theoretical conservative VF risk with XRF or X2 CEW to be less than 0.76 ppm (III.E). This is significantly lower than either the fatal fall (5.3 ppm) or fatal burn (1.9 ppm) risks, or much lower than the combined 7.2 ppm non-cardiac mortality risk. Comparison with other epidemiological and risk assessment studies have been provided in our previous [1, 29]. They are applicable to and consistent with results of this current study.

V. Conclusions

To-date, there has been no undisputed medical evidence linking causation of VF to use of CEWs. In general, CEWs should not be considered risk-free force options. The new XRF and X2 CEWs have extremely low cardiac risk profiles and exhibit increased cardiac safety margins over the previously analyzed X26 CEW model. Their estimated theoretical conservative risk of VF induction, even when considering effects of premature ventricular responses, is likely to be significantly less than 1 in more than 1.3 million cases, much lower than non-cardiac risk levels associated with use of CEWs.

References

[1] D. Panescu, M. Kroll and M. Brave, "Cardiac Fibrillation Risks with TASER Conducted Electrical Weapons," *Conf Proc IEEE Eng Med Biol Soc*, vol. 2015, pp. 323-329, 2015.

[2] M. H. Nerheim, Systems and methods for an electronic control device with date and time recording, US Patent 7,570,476, August 4, 2009.

[3] TASER International: Smart Weapons Technology. Available at https://www.taser.com/products/smart-weapons.

[4] J. Ho, D. Dawes, J. Miner, S. Kunz, R. Nelson and J. Sweeney. "Conducted electrical weapon incapacitation during a goal-directed task as a function of probe spread," Forensic Sci Med Pathol, vol. 8(4), pp. 358-366, 2012.

[5] H. Sun. Models of ventricular fibrillation probability and neuromuscular stimulation after Taser® use in humans. PhD thesis: University of Wisconsin, 2007. Available online: http://ecow.engr.wisc.edu/cgi-bin/get/ece/762/webster/

[6] H. Sun, J. Y. Wu, R. Abdallah and J. G. Webster, "Electromuscular incapacitating device safety," *Proc IFMBE*, 3rd EMBE Conference, Prague, vol. 11(1), 2005.

[7] L.A. Geddes and L. E. Baker. Principles of Applied Biomedical Instrumentation, 3rd Ed. New York: John Wiley & Sons, 1989.

[8] J. A. Pearce, J. D. Bourland, W. Neilsen, L. A. Geddes and M. Voelz, "Myocardial stimulation with ultra-short duration current pulses," *PACE*, vol. 5(1), pp. 52-8, 1982.

[9] R. H. Zoll, P. M. Zoll and A. H. Belgard, "Noninvasive cardiac stimulation," In G. A. Feruglio, Ed: *Cardiac pacing: electrophysiology and pacemaker technology*, pp 593-596, Padua: Piccin Medical Books, 1983.

[10] W. D. Voorhees, K. S. Foster, L. A. Geddes and C. F. Babbs, "Safety Factor for Precordial Pacing: Minimum Current Thresholds for Pacing and for Ventricular Fibrillation by Vulnerable-Period Stimulation, *PACE*, vol. 7, pp. 356–360, 1984.

[11] Sugimoto, Schaal, and Wallace, "Factors determining vulnerability to ventricular fibrillation induced by 60-cps alternating current," *Circ Res*, vol. 21, pp. 601-608, 1967.

[12] International Electrotechnical Commission, Effects of current on human beings and livestock: Part 1 – General aspects, IEC 60479-1, 2005, Geneva: IEC.

[13] International Electrotechnical Commission, Effects of current on human beings and livestock: Part 2 – Special aspects, IEC 60479-2, 2007, Geneva: IEC.

[14] Structural Research & Analysis Corporation (SRAC), division of SolidWorks Corporation, COSMOS/M: http://www.cosmosm.com/pages/products/cosmosm.html

[15] J. P. Delille, A. Hernigou, V. Sene, G. Chatellier, J. C. Boudeville, P. Challande and M. C. Plainfosse, "Maximal thickness of the normal human pericardium assessed by electron-beam computed tomography," *Eur Radiol*, vol. 9(6), pp. 1183-9, 1999.

[16] R. S. Gautam, G. V. Shah, G. V., H. R. Jadav and B. J. Gohil, "The Human Sternum – as An Index of Age & Sex," *J Anat Soc India*, vol. 52(1), pp. 20-23, 2003.

[17] Lumen Cross-Sectional Tutorial by John McNulty: http://www.meddean.luc.edu/lumen/MedEd/grossanatomy/x_sec/main x_sec.htm

[18] D. Panescu, M.W. Kroll, C. Iverson, M. Brave, "Electrical Shielding Effects of the Sternum," *Conf Proc IEEE Eng Med Biol Soc*, vol. 2014, pp. 4464-70, 2014

[19] D. Panescu, J. G. Webster and R. A. Stratbucker, "A nonlinear finite element model of the electrode-electrolyte-skin system," *IEEE Trans Biomed Eng*, vol. 41(7), pp. 681–687, 1994.

[20] D. Panescu, J. G. Webster, W. J. Tompkins and R. A. Stratbucker, "Optimization of cardiac defibrillation by three-dimensional finite element modeling of the human thorax," *IEEE Trans Biomed Eng*, vol. 42(2), pp. 185–192, 1995.

[21] S. Singh and S.Saha, "Electrical properties of bone. A review," *Clin Orthop Relat Res*, vol. 186, pp. 249-71, 1984.

[22] J-Y Wu, H, Sun, A, O'Rourke, S. Huebner, P. S. Rahko, J. A. Will and J. G. Webster, "TASER dart-to-heart distance that causes ventricular fibrillation in pigs," *IEEE Trans Biomed Eng*, vol. 54, pp. 503-508, 2007.

[23] G. G. Bashian; G. A. Wagner; D. W. Wallick and P. J. Tchou, "Relationship of Body Mass Index (BMI) to Minimum Distance from Skin Surface to Myocardium: Implications for Neuromuscular Incapacitating Devices (NMID)", *Circulation*, vol. 116:II, pp. 947, 2007.

[24] S. J. Stratton, C. Rogers, K. Brickett and G. Gruzinski, "Factors associated with sudden death of individuals requiring restraint from excited delirium," *Am J Emerg Med*, vol. 19, pp. 187-191, 2001.

[25] M. White, J. Ready, C. Riggs, D. M. Dawes, A. Hinz and J. D. Ho, "An Incident-Level Profile of TASER Device Deployments in Arrest-Related Deaths," *Police Quarter*ly, vol. 16, no. 1, pp. 85-112, 2013

[26] W. P. Bozeman, E. Teacher and J. E. Winslow, "Transcardiac conducted electrical weapon (TASER) probe deployments: incidence and outcomes," *J Emerg Med*, vol. 43(6), pp. 970-975, 2012.

[27] J. E. Brewer, M. W. Kroll, "Field Statistics Overview," in TASER® Conducted Electrical Weapons: Physiology, Pathology, and Law, M.W. Kroll, J.D. Ho Eds., Springer, 2009.

[28] M. W. Kroll, J. Adamec, C. V. Wetli and H. E. Williams, "Fatal traumatic brain injury with electrical weapon falls*," Journal of Forensic and Legal Medicine*, vol. 43, pp. 12-19, 2016.

[29] M. A. Brave, M. W. Kroll, S. Karch, C. Wetli, M. Graham, S. Kunz, D. Panescu, "Medical Examiner Collection of Comprehensive, Objective Medical Evidence for Conducted Electrical Weapons and Their Temporal Relationship to Sudden Arrest," *World Academy of Science, Engineering and Technology, International Science Index, Law and Political Sciences*, vol. 3(1), p. 527, 2017.

[30] C. Clarke and S. Andrews, "The ignitability of petrol vapours and potential for vapour phase explosion by use of TASER® law enforcement electronic control device," *Science & Justice*, vol. 54, pp. 412-420, 2014.

Authorized licensed use limited to: Charles University. Downloaded on October 10,2025 at 23:49:05 UTC from IEEE Xplore. Restrictions apply.